# XI. RAMAN SPECTROSCOPY

References:


- D.C. Harris och M.D. Bertolucci, Symmetry and Spectroscopy, Oxford University Press, 1978.
- J. M. Hollas, Modern Spectroscopy, Wiley, Chichester, 1987.
- Handbook of vibrational spectroscopy, J. M. Chalmers, P. R. Griffiths, Ed.'s, Wiley, 2002.
- G. Herzberg, Infrared and Raman Spectra, Van Nostrand, 1945.
- K. P. Huber och G. Herzberg, Constants of Diatomic Molecules, Van Nostrand, 1979.
- P.W. Atkins, Molecular Quantum Mechanics, Oxford University Press, 1983.
- L.A. Woodward, Introduction to the Theory of Molecular Vibrations and Vibrational Spectroscopy, Clarendon Press, 1972.
- E.B. Wilson, J.C. Decius och P.C. Cross, Molecular Vibrations, McGraw-Hill, 1955. (En ny upplaga: Dover, 1980).
- S. Califano, Vibrational States, Wiley, 1976.
- E.F.H. Brittain, W.O. George och C.H.J. Wells, Academic Press, 1970.
- M.D. Harmony, Introduction to Molecular Energies and Spectra, Holt & Winston, 1972.
- CRC Handbook of Spectroscopy.
- T. Hase, Spektrometriset taulukot, Otakustantamo, 1984. CRC Press, 1999.
- B. Schrader, Raman/infrared atlas of organic compounds, VCH, Weinheim, 1989.
- D. A. Long, The Raman effect. A unified treatment of the theory of Raman scattering by molecules, Wiley, Chichester, 2002.


drafted by
Prof. Matti Hotokka
Åbo Akademi University
Department of Physical Chemistry
Turku (Finland)

# XI.1. The Raman phenomenon

The Raman spectroscopy measures the **vibrational motions** of a molecule like the infrared spectroscopy. The physical method of observing the vibrations is, however, different from the infrared spectroscopy. In **Raman spectroscopy** one measures the **light scattering** while the infrared spectroscopy is based on absorption of photons. A summary of the scattering theory is given in Appendix I. Scattering is also discussed in advanced textbooks in quantum mechanics.

The Raman phenomenon was detected in 1928 by the Indian physicist Sir Chandrasekhara Venkata Raman and Kariamanikkam Srinivasa Krishnan.[1][2] Independently of this work, the phenomenon was also reported by Grigory Landsberg and Leonid Mandelstam.[3] However, the phenomenen was predicted theoretically even earlier by using the classical model.[4] After the end of 1920's the method was forgotten for several decades because the signal is very weak. Raman spectrocopy experienced a renaissance in the 1960's when the lasers were invented and started to be used as light sources in spectroscopy.

The basics of the Raman scattering can be explained using classical physics but a more comprehensiv theory requires quantum mechanical treatise. Both the classical and quantum mechanical formulations are schetched below.

### Classical description of the Raman phenomenon

Consider a molecule (for the sake simplicity one) without a permanent dipole moment. The effect of a permanent dipole moment can be easily incorporated. An oscillating electric field

$$\mathbf{F} = \mathbf{F}_0 \cos(\nu_0 t) \tag{XI.1}$$

induces a dipole moment

$$\mu = \alpha \mathbf{F}_0 \cos(\nu_0 t). \tag{XI.2}$$

The quantity $\alpha$ is the **polarizability** of the molecule. The polarizability is not a constant but varies with every vibrational motion of the molecule. Let the fundamental vibration

[1] C. V. Raman and K. S. Krishnan, *Nature*, **121** (1928) 501 - 502, "A new type of secondary radiation"; C. V. Raman and K. S. Krishnan, *Indian Journal of Physics* **2** (1928) 399 - 419, "A new class of spectra due to secondary radiation. I.".

[2] C. V. Raman was made a knight in 1929 and received the Nobel proce for his invention in 1930.

[3] G. Landsberg and L. Mandelstam, *Naturwiss.* **16** (1928) 557 - 558.

[4] A. Smekal, *Naturwiss.* **16** (1923) 873.

frequences of the molecule be $\nu_k$, $k = 1, 2, \ldots, M$. Then

$$\alpha = \alpha_0 + \sum_{k=1}^{M} \alpha_k \cos(\nu_k t + \phi_k). \tag{XI.3}$$

A phase factor $\phi_k$ has been included in the formula. The induced dipole moment is

$$\begin{aligned} \mathbf{p} &= \alpha_0 \mathbf{F}_0 \cos(\nu_0 t) + \sum_{k=1}^{M} \alpha_k \mathbf{F}_0 \cos(\nu_0 t) \cos(\nu_k + \phi_k) \\ &= \alpha_0 \mathbf{F}_0 \cos(\nu_0 t) \\ &\quad + \sum_{k=1}^{M} \alpha_k \mathbf{F}_0 \big\{ \cos[(\nu_0 + \nu_k)t + \phi_k] + \cos[(\nu_0 - \nu_k)t + \phi_k] \big\}. \end{aligned} \tag{XI.4}$$

The classical theory of electromagnetism states that an oscillating dipole emits radiation of the intensity

$$I = \frac{\nu_0^4}{12\pi\epsilon_0 c^3} |p|^2. \tag{XI.5}$$

A simple insertion gives the result

$$\begin{array}{lll} I = & \frac{\nu_0^4}{12\pi\epsilon_0 c^3} \alpha_0^2 \mathbf{F}_0^2 \cos^2(\nu_0 t) & \text{Rayleigh} \\ & + \frac{1}{12\pi\epsilon_0 c^3} \sum_{k=1}^{M} \alpha_k^2 \mathbf{F}_0^2 \times \{ (\nu_0 + \nu_k)^4 \cos^2[(\nu_0 + \nu_k)t + \phi_k] & \text{anti} - \text{Stokes} \\ & \quad + (\nu_0 - \nu_k)^4 \cos^2[(\nu_0 - \nu_k)t + \phi_k] \} & \text{Stokes} \\ & + \ldots & \end{array} \tag{XI.6}$$

An oscillating dipole moment emits therefore with the frequency of the incident field (**Rayleigh scattering**) in phase with the incident field. In addition, the molecule radiates with two frequencies that are modulated by the frequency of the excited normal vibration and phase shifted (**Raman scattering**). The Raman scattered light has a lower frequency than the incident light (**Stokes-raman scattering**) or a higher frequency (**anti-Stokes-Raman scattering**).

One of the failures of the classical picture is that the ratio of the Stokes and anti-Stokes intensities should theoretically be

$$\frac{I(\text{Stokes})}{I(\text{anti} - \text{Stokes})} = \frac{(\nu_0 - \nu_k)^4}{(\nu_0 + \nu_k)^4}, \tag{XI.7}$$

which is not the case experimentally.

**The quantum mechanical description of the Raman effect**

The relevant quantum mechanical system is the molecule plus the field. Usually the time-dependent Schrödinger equation of the system is solved by using perturbation theory, basically in the same way the Einstein transition rate is calculated, but in this case to second order. The intensities are then according to Appendix I

$$I_i^{nm} = \frac{4e^4}{16\pi^2\epsilon_0^2 c^4}(\nu_0 \pm \nu_k)^4 | < n|m_i|m > |^2 \tag{XI.8}$$

with the matrix elements of the induced dipole moment

$$\begin{aligned} < n|m_i|m > = \frac{\pi}{h} \sum_j \sum_r \{ & \frac{< n|\hat{\mu}_i|r >< r|\hat{\mu}_i \hat{F}_j^0|m >}{\nu_{rm} - \nu_0} \\ & + \frac{< n|\hat{\mu}_i \hat{F}_j^0|r >< r|\hat{\mu}_i|m >}{\nu_{nr} - \nu_0} \}. \end{aligned} \tag{XI.9}$$

The momentaneous dipole moment $\hat{\mu}_i$ is determined also here by the polarizability. The meaning of this expression is illustrated in Fig. XI.1. In addition to the free molecule's eigenstates (somewhat perturbed) the system also has (an infinite number of) virtual states r. Very schematically one can say that the molecule is excited to a virtual state where a photon has transferred from the electric field to the molecule ("*dressed molecule*") and then goes back to one of the initial states. In the figure it is also shown that the energy of the incident photon must not be equal to any of the electronic excitation energies of the molecule because the photon is absorbed in that vase. The uppermost whole line in the figure indicates an electronically excited state.

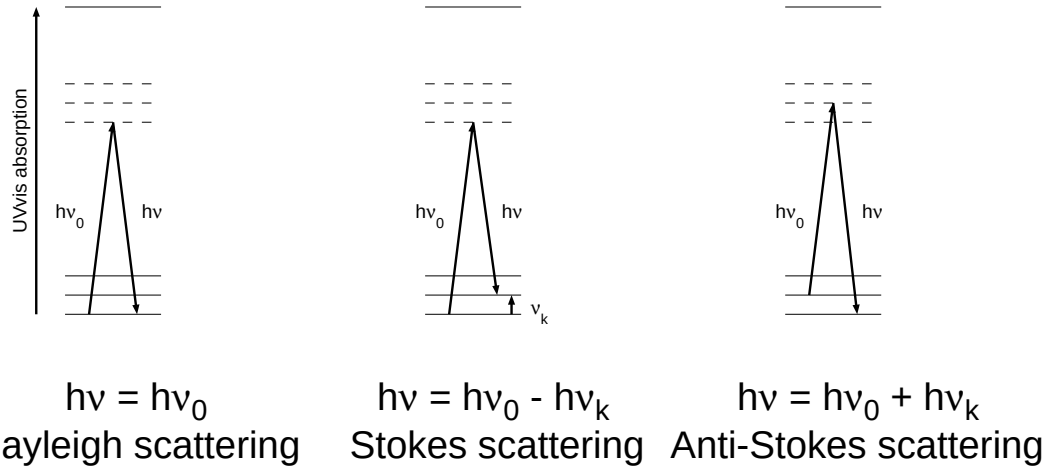


Fig. XI.1. Schematic representation of the Raman effect.

In the quantum mechanical model the intensity depends on the occupation of the initial state. This is determined by the Boltzmann distribution. Thus the intensity ratio is

$$\frac{I(\text{Stokes})}{I(\text{anti}-\text{Stokes})} = \frac{(\nu_0 - \nu_k)^4}{(\nu_0 + \nu_k)^4} e^{hc\tilde{\nu}_k/kT}. \tag{XI.10}$$

This ratio depends on the temperature $T$. Therefore one can determine the temperature of the sample by measuring the intensities of both the Stokes line and the corresponding anti-Stokes line. The **temperature** is given by the formula

$$T = \frac{-\tilde{\nu}_k \times 1.43879}{[\ln\{\frac{I(\text{anti}-\text{Stokes})}{I(\text{Stokes})}\} + 4\ln\{\frac{\nu_0-\nu_k}{\nu_0+\nu_k}\}]}. \tag{XI.11}$$

An example of the Raman spectrum is shown in Fig. XI.2.

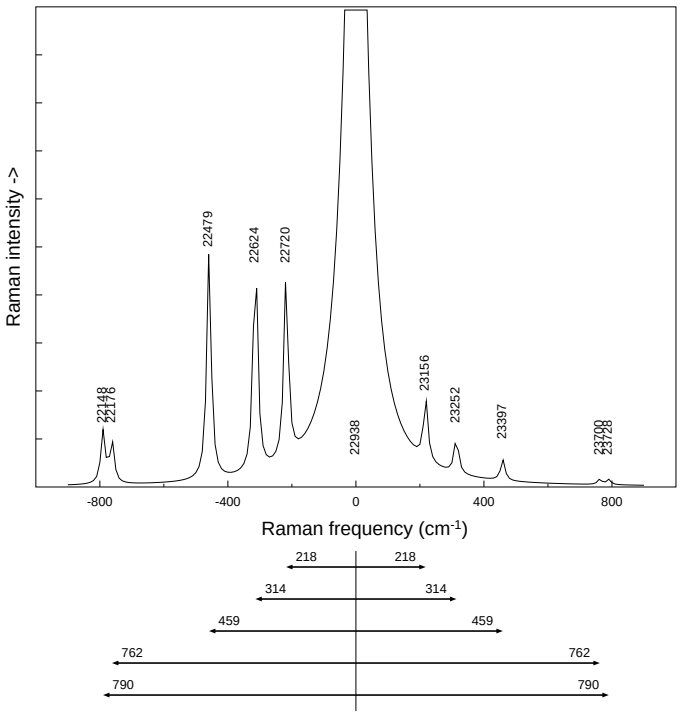


Fig. XI.2. An example of a Raman spectrum. Carbon tetrachloride.

## Intensity of the scattered light

The most common process in light scattering is that the photon does not interact at all with the sample but simply passes through it. Only one photon of $10^3$ or $10^4$ is scatteted.

An overwhelming majority of the scattered photons show Rayleigh scattering where the frequency of the scatteted light is the same as that of the incident light. Only one of a thousand or ten thousand scattered photons will have a modulated frequency, *i.e.* will be Raman scattered. Therefore the intensity of the Rayleigh signal is a thousandth of the intensity of the incident light and **intensity of the Raman signal** is a millionth of the intensity of the incident light.

In the above figure the Rayleigh band is shown in the middle. Its frequency $\nu_0$ is used as the origin of the Raman spectrum. The positions of the Raman bands are $\nu_0 \pm \nu_k$. Their displacements from $\nu_0$ give the frequencies of the normal vibrations. The Rayleigh band is very intense as compared to the Raman bands on both sides of it. The Stokes-Raman bands on the low-energy side are stronger than the anti-Stokes-Raman bands on the high-energy side of the central Rayleigh band but their distances from the central band are the same as those of the Stokes-Raman bands. In practical measurements one wishes to remove the strong rayleigh band in order to be able to observe the Raman signals. Therefore only the Stokes-Raman part of the spectrum is usually shown. The infrared and Raman spectra of carbon tetrachloride are shown in Fig. XI.3.

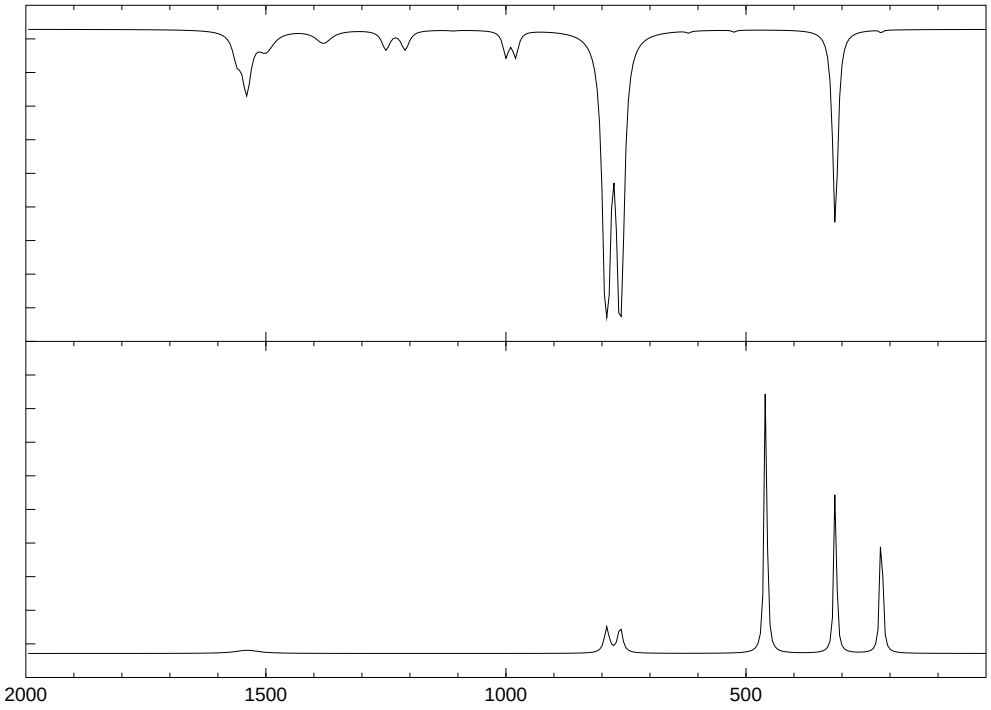


Fig. XI.3. Infrared and Raman spectra of carbon tetrachloride.

The intensity of the signal is determined by the **scattering cross section** $\sigma(\theta, \phi; \nu)$, by the frequency of the incident light and by the Boltzmann factor. The scattering cross section depends on the molecular polarizability tensor $\alpha$, see Appendix I. From this follow the selection rules in the Raman spectroscopy. The effect of the incident light is important because the intensity depends on the fourth power of the frequency. If the wavelength is

halved (*e.g.*, from 1064 to 532 nm) the intensity of the scattered light will increase by a factor 16.

# XI.2. The Raman spectrometer

### The light source

The light source of a Raman spectrometer must give very intense radiation for the scattered light to be strong enough to be observed. In addition, the light should be as monochromatic as possible so that the Raman bands would be as narrow as possible.

In the old instruments a **mecury vapor lamp** is commonly used. It has several strong emission bands (253.7, 365.4, 404.7, 435.8, 546.1 and 578.0 nm). If one does not use a filter to select one of the bands all of them will generate a spectra that may partly overlap. The emission bands also have quite large widths which will be convoluted into the resulting Raman spectrum and result in quite broad Raman bands. The emission bands of a mercury lamp lie in the range from UV to visible green light. This is very favorable in Raman spectroscopy because the intensity of the scattered light inreases with the fourth power of the frequency. On the other hand one risks to hit on an electronic absorption band which will result in fluorescence. The fluorescence in Raman spectroscopy is discussed in detail later. In modern spectrometers a **laser** is used as the light source because it gives a high intensity and the light can easily be focused in a small spot in the sample. Laser light is also polarized and this can be used to determine the depolarization ratio. Gas lasers, in particular the argon laser that has two stron emission lines at 514 and 488 nm, have been popular. In FT-Raman spectrometers Nd:YAG lasers with an emission wavlength of 1064 nm are popular. Today, also diode lasers are gaining popularity. Diode lasers can have one of several emission wavelength, in particular 976, 830 and 785 nm are popular. The emission power of modern diode lasers is typically several hundred milliwatts.

### The sample

The scattered light is distributed in all directions. Two **observation geometries** are particularly popular. For liquid samples observation at 90° angle to the incident light beam is used most often. This geometry is shown schematically in Fig. XI.4. Ine can also observed light that is scattered in 180° angle (**back scattering**). This is normally the only possibility for solid samples. Both geometries have their good points. The optical arrangement is simpler in the 90° geometry. Also, the portion of Raman scattering of all the scattered light is larger in 90° geometry than in 180° geometry. For gaseous nitrogen

the ratios are[5]

$$\frac{I_{Raman}(90°)}{I_{Rayleigh}(90°)} = 1.32 \times \frac{I_{Raman}(180°)}{I_{Rayleigh}(180°)}. \tag{XI.12}$$

In the 180° geometry one only needs to have access to one surface of the sample which may make the practical experiment easier. The scattering intensity is also highest at 180°. For gaseous nitrogen

$$\frac{I_{Raman}(180°)}{I_{Raman}(90°)} = 1.50. \tag{XI.13}$$

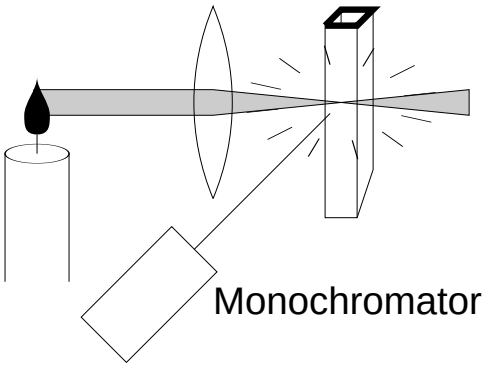


Fig. XI.4. Raman experiment at 90° geometry.

The estimates above are based on the following scattering probabilities at angle $\theta$,

$$\begin{aligned} P_{Rayleigh}(\theta) &= 0.75 \times (1 + \cos^2\theta) \\ P_{Raman}(\theta) &= \left[\frac{3}{4+8\rho}\right] \left[1 + 3\rho + (1-\rho)\cos^2\theta\right]. \end{aligned} \tag{XI.14}$$

Here $\rho$ is the depolarization ratio. For nitrogen, $\rho = 0.19$ when the wavelength of the incident light is 337.1 nm. One can also derive for nitrogen gas the relation

$$\frac{I_{Raman}(180°)}{I_{Rayleigh}(180°)}) = 4.9 \times 10^{-4}. \tag{XI.15}$$

The sample cell is often an nmr tube or a capillary tune that is made of suitable glass grade. The laser light is focused on the sample so that the glass wall of the cell does not disturb the experiment. The scattered light is collected by using a large condensing lense and directed to a monochromator or an interferometer and thence to the detector.

[5] N. M. Reiss, *J. Appl. Phys.* **43** (1972) 739.

### Monochromator and interferometer

In the infrared spectoscopy the interferometric technique has completely replaced the dispersive technique. In Raman spectroscopy, however, the **dispersive spectrometers** have certain advantages over the interferometry. The largest manufacturers of FT-Raman spectrometers also produce dispersive Raman spectrometers. The dispersive instruments are significantly more sensitive (by a factor of ten to hundred) than the FT-Raman spectrometers. Therefore smaller laser effects can be used and thereby sensitive samples are affected less. They also have a lower noise level indicating a lower detection limit. In an FT-Raman spectrometer the dominating source of noise is the detector noise while in modern dispersive Raman spectrometers the **shot noise** (*i.e.*, random fluctuations of the charge carriers in the electronic circuits) dominates. It is also easier to change the wavelength of the incident light in a dispersive spectrometer than in an FT-Raman spectrometer in case the measurement is disturbed by, *e.g.*, fluorescence. Today CCD detectors are common. They make the measurements fast because the whole spectrum (or a large portion of it) can be measured simultaneously.

One of the great challenges in Raman spectroscopy is to remove the Rayleigh signal. This is accomplished in the old spectrometers by using very large **double** or **triple monochromators** with large focal lengths (up to 1 m) and very high resolution. This allows the recording of spectra quite close to the central burst without the Rayleigh signal reaching to the detector. The optical arrangement of a typical double monochromator is shown in Fig. XI.5.[6] The two gratings must be turned in phase and therefore the structure of the monochromator is such that both gratings are fixed to a common axis.

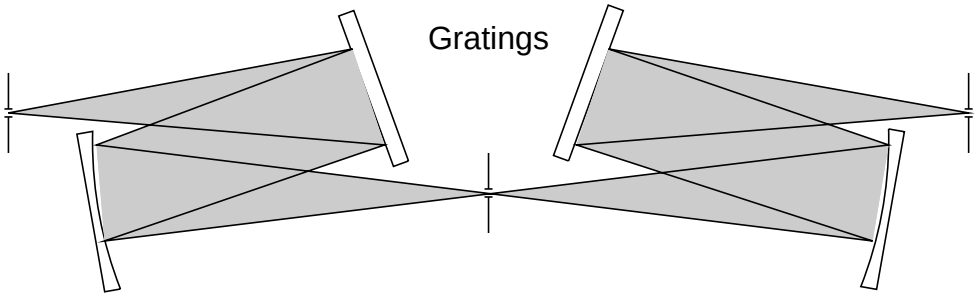


Fig. XI.5. A double monochromator schematically (Solar TII DM160).

A traditional triple monochromator is shown in Fig. XI.6. The illustration shows schematically McPherson's McTriple LE monochromator,[7] the two first stages of which are 20 cm ononchromators with gratings that are rotated simultaneously by a connecting rod. The

[6] http://solartii.com/

[7] http://www.mcphersoninc.com/ramanspectroscopy/McTripleLE.htm

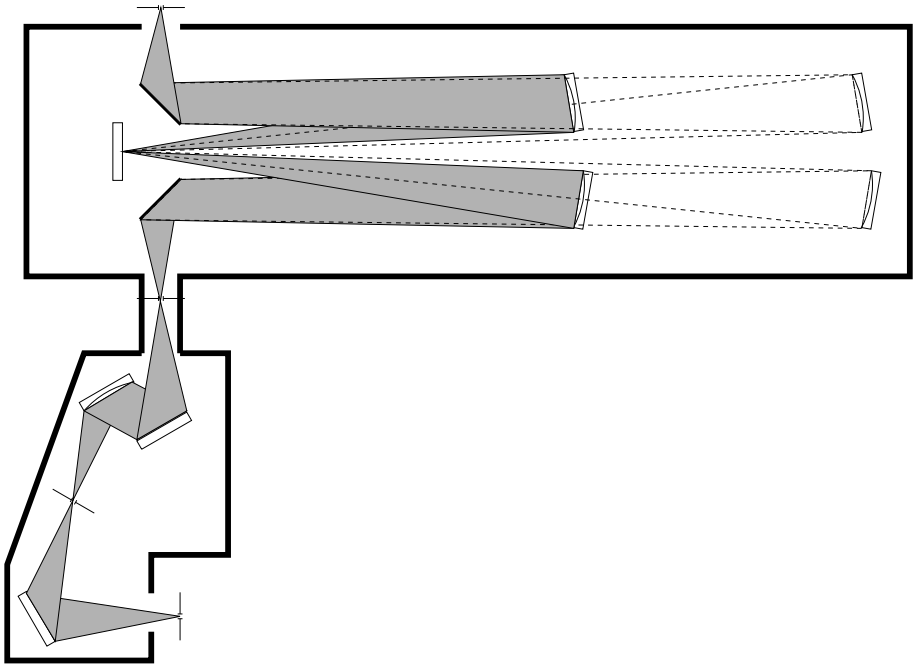

Fig. XI.6. A triple monochromator schematically. (McPherson McTripple LE).

focal length of the third stage is either 67 or 133.5 cm. The apertures are f/4.8 and f/9.4, respectively.

The success of the interferometric technique in infrared spectroscopy has also led to manufacturing of commercial **FT-Raman spectrometers**. They are often accessories to infrared spectrometers. One such construction is shown schematically in Fig. XI.7. Pure FT-Raman spectrometers are also produced. They are often modifications of existing FTIR spectrometer benches. The interferometric technique is demanding in the short wavelength range and in particular in the UV region. The FT-Raman spectrometers are usually equipped with an Nd:YAG laser emitting near infrared light and with an effect of up to 1 W. Diode lasers are becoming more popular. They work ususally at 976 or 785 nm wavelengths. An instrument may be equipped with several diode lasers in order to be able to avoid fluorescence.

The most critical component in an FT-Raman spectrometer is the **filter** that damps the Rayleigh scattered light as the interferometer cannot do this. If the Rayleigh light reaches to the detector, the detector will be overflown. On the other hand, the the Raman signals close to the Rayleigh band must be observed. This poses high requirements on the filter. A holographic **notch filter** with an optical denisty of at least 6[8] and a bandwidth of $\pm 100$ $cm^{-1}$ is used. Each laser type must have a filter that is specifically optimized for the appropriate laser wavelength. A typical transmission curve is shown in Fig. XI.8.

[8] Opticalsk density is defined here as $OD = -\log_{10}(Transmission)$. An alternative definition is $OD = -\log_{10}(Transmission)/l$.

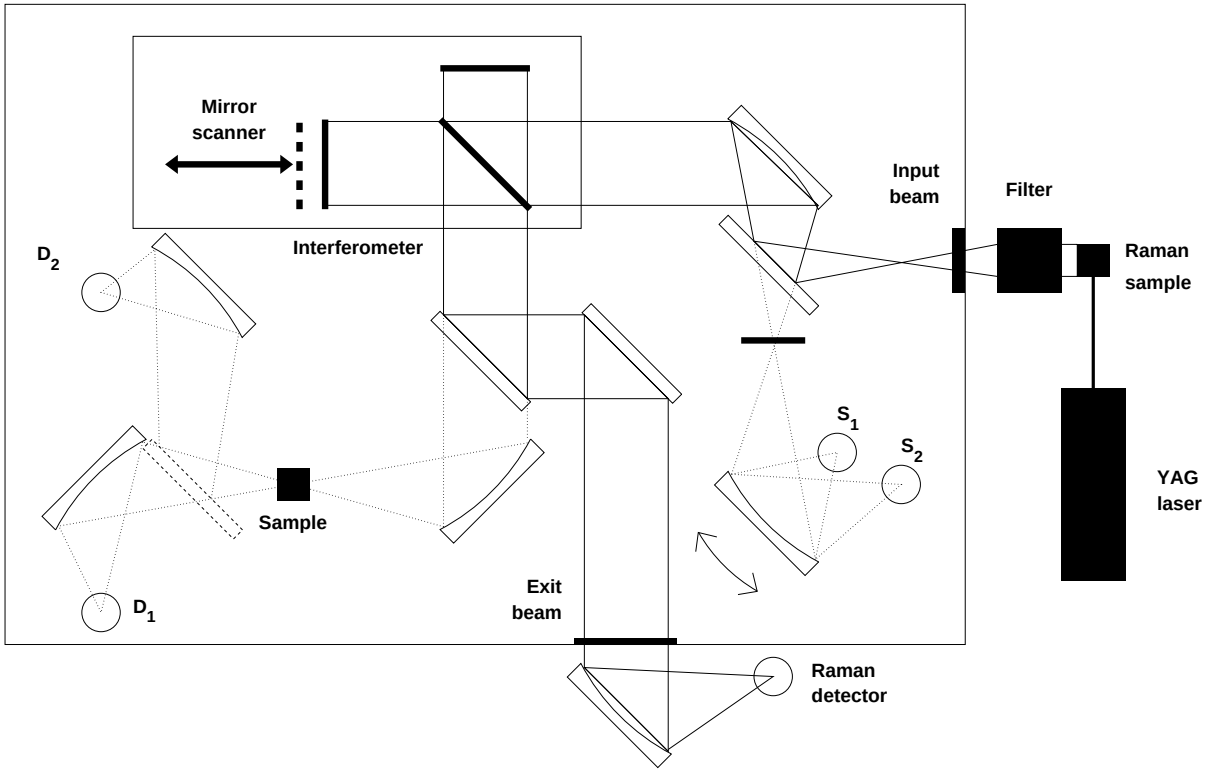


Fig. XI.7. FT-Raman module attached to Bruker IFS66.

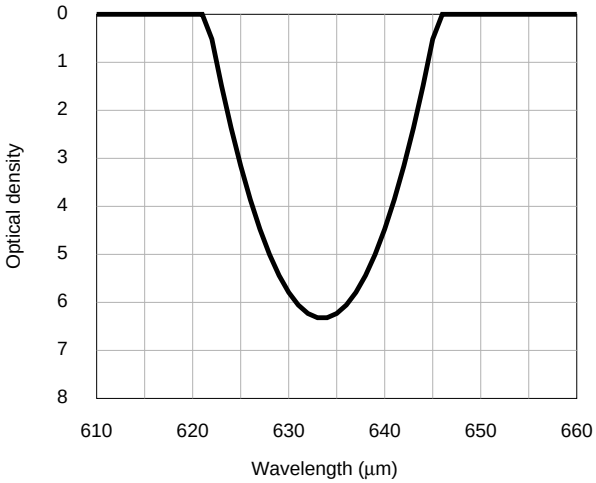


Fig. XI.8. Transmission curve of a notch filter. It is assumed here that the wavelength of the laser light is 633.5 nm.

The **detectors** used in the FT-Raman spectroscopy depend on the laser wavelength. The Raman signal is extremely weak and therefore the detector must be sensitive and its noise level low. The most common detector type is the germanium detector the must, however, be cooled down wit liquid nitrogen. It is excellent when used with a Nd:YAG laser. Examples of detector types that can be used in the near infrared region are shown in Fig.

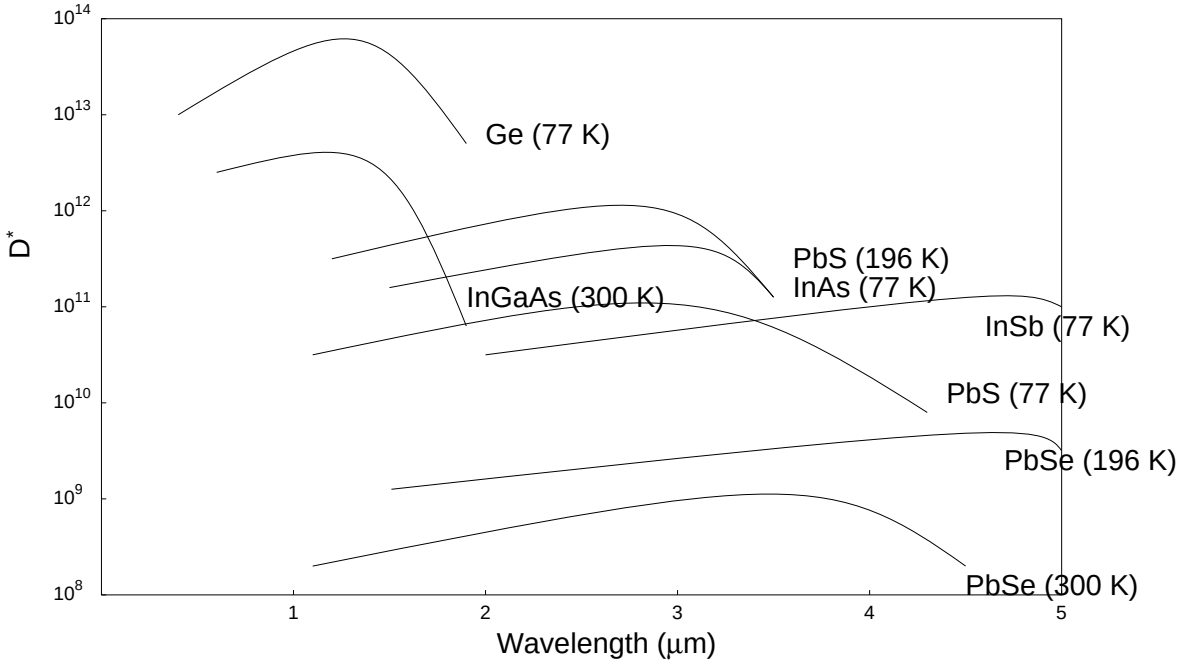


Fig. XI.9. Examples of detectors for the NIR region.

XI.9.

The modern **dispersive spectrometers** use filters similar to those in FT-Raman spectrometers. Then one can use a rather small monochromator as it does not need to separate away the Rayleigh band. On the other hand, the filter is optimized for a particular laser type. If one wishes to have several lasers to choose among then one also has to implement all the necessary filters in the spectrometer. The most common detector type is a **CCD detector** that allows a fast uptake of the whole spectrum. At low resolution one does then not need any moving parts in the spectrometer. The whole spectrum is recorded simultaneously. This technique is also excellent for new measuring methods such as mapping. The principle of such specttrometers is illustrated in Fig. XI.10.

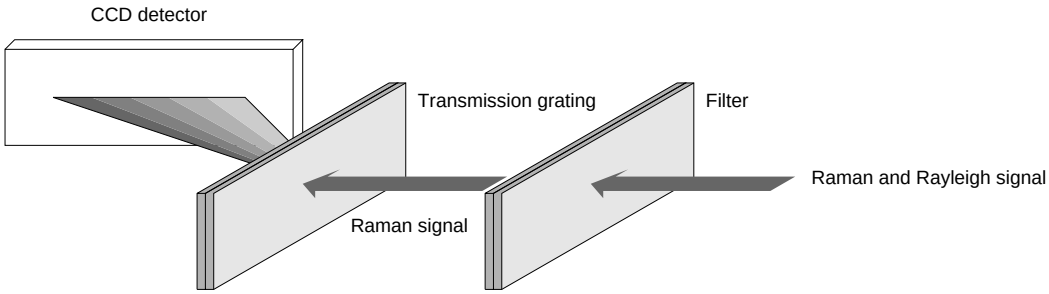


Fig. XI.10. Dispersive Raman spectroscopy using a transmission grating.

# XI.3. Selection rules in Raman spectroscopy

Raman spectroscopy measures molecular vibrations. The actual vibrations are the same as in infrared spectroscopy and their **symmetries** can be determined in the same way as in infrared spectroscopy. This procedure has been discussed in chapter VII. The **selection rules** can thus be derived from the theory of point groups. The physical interaction mechanism in infrared spectroscopy is absorption of photons. That process is determined by the fluctuations of the electric dipole moment of the molecule. In Raman spectroscopy the photons are scattered. The physical quantity that governs scattering is the polarizability. In all other respects the analysis is similar to that in infrared spectroscopy. The principles for both experimental techniques have been discussed in chapter VII. The basic principles for interpretation of Raman spectra are discussed below.

The intensity of the scattered light depends on the **differential scattering cross section** $\sigma(\theta, \phi)$. Molecules with an easily polarizable electron cloud have a high scattering cross section. In Raman spectroscopy the vibrations affect the polarizability and therefore different vibrational modes give different band intensities. The intensity of the Raman signal is strongly affected by the frequency of the incident light. Therefore one often uses the **reduced scattering cross section** $\sigma(\theta, \phi)(\tilde{\nu}_0 - \tilde{\nu}_k)^{-4}$. The reduced scattering cross sections of a few liquids are shown in the table below. Wavelength of the incident light is 488 nm.

| Molekyl | Vibration ($cm^{-1}$) | $\sigma(\theta, \phi)(\tilde{\nu}_0 - \tilde{\nu}_k)^{-4}$ $10^{-48}$ $cm^6/sr$ |
|---|---|---|
| $C_6H_6$ | 992 | 225 |
| $C_6H_5CH_3$ | 1002 | 127 |
| $C_6H_5NO_2$ | 1345 | 766 |
| $CS_2$ | 656 | 280 |
| $CCl_4$ | 459 | 140 |
| $CHCl_3$ | 666 | 54 |
| | 762 | 32 |
| $C_6H_{12}$ | 802 | 60 |

Molecules with **aromatic** or conjugated functional groups show a high Raman intensity because the delocalized electrons are easily polarizable. Molecules with double bonds or free electron pairs often show hifh Raman signals. However, water is a notable exception. There the free electron pairs form hydrogen bonds and their polarizability is reduced. *Water is a good solvent in Raman spectroscopy.* The complexes of transition metal ions often give strong Raman signals.

Molecules can rotate and the rotational transitions can be observe both in absorption and scattering spectra. The term rotational spectroscopy refers to absorption spectroscopy because the pure rotational bands are difficult to observe in Raman spectroscopy as they are very weak and lie very close to the Rayleigh band. This is shown schematically in Fig. XI.11.

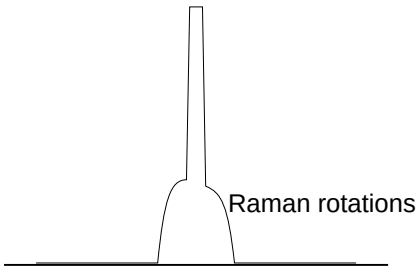


Fig. XI.11. Raman rotations schematically.

The rotational motions can also be observed as fine structure of the vibrational bands. Normally, one can only observe that the vibrational bands are broad. The rotational levels have so low energies that the ambient thermal energy can cause transitions. The band width is determined by the Boltzmann distribution. If the sample is cooled down to 4 K the vibrational bands are quite narrow both in infrared and Raman spectroscopy.

In infrared spectroscopy the selection rule for the rotational transitions is $\Delta J = 0, \pm 1$, which give rise to the $P$, $Q$ and $R$ branches. In Raman spectroscopy the corresponding selectiion rules are $\Delta J = 0, \pm 2$ and the labels of the branches are then $O$, $Q$ and $S$.

# XI.4. Interpretation of Raman spectra

The selection rules of Raman spectroscopy are different from those of inrared spectroscopy because the physical processes givin rise to the spectra are different. However, the actual molecular vibrations are the same. Therefore the basic principles of **assignment** are the same in infrared and Raman spectroscopy. If a vibrational motion is active in both infrared and raman spectroscopies the band position is obviously the same in both spectra. The difference of the selection rules can result in bands that are strong in the infrared spetrum but weak in the Raman spectrum and *vice versa*. Therefore the infrared and Raman spectra differ and the same correlation tables cannot be used for both. The two methods complement each other.

The Raman spectra are often simpler than the corresponding infrared spectra. The allowed fundamental transitions give very strong signals while the forbidden fundamental transitions often give very weak signals in Raman spectroscopy. This is typically not the case in infrared spectroscopy.

Certain functional groups are easily identified from the infrared spectrum and others in the Raman spectrum. One notable example of the differences are the sceleton vibrations of aromatic hydrocarbons. Some examples are shown in the table below.

| Molecule | Band position $cm^{-1}$ | Intensity Raman | IR |
|---|---|---|---|
| Naphtalene | 1630 - 1595 | w | m |
| | 1580 - 1570 | vs | vw |
| | 1510 - 1500 | vw | m |
| | 1390 - 1350 | vs | ms |
| Anthracene | 1630 - 1620 | ms | ms |
| | 1560 - 1550 | vs | s |
| | 1400 - 1390 | vs | vw |
| Fenantrene | 1620 - 1600 | m | m |
| | 1520 - 1500 | m | s |
| | 1460 - 1440 | s | m |
| | 1350 - 1300 | vs | w |

One application where Raman spectroscopy can be particularly useful is identification of inorganic compounds that often have low vibrational frequencies lying close to or even below 400 $cm^{-1}$ which is the limit for infrared spectroscopy. Some examples of the Raman spectra of inorganic three, four and five atom ions are shown in the table below. The

symbol $p$ indicates that the band is polarized.

| Molecule (puktgrupp) | $\nu_1$ band, $cm^{-1}$ (vibration, symmetry) | | | | $\nu_2$ band, $cm^{-1}$ (vibration, symmetry) | | | |
|---|---|---|---|---|---|---|---|---|
| | in $H_2O$ | powder | R | IR | in $H_2O$ | powder | R | IR |
| $D_{\infty h}$ | | $\nu_s(\Sigma^+)$ | | | | $\delta(\Pi)$ | | |
| $NO_3^-$ | 1350 | 1380 - 1320 | vs | | 635 | 660 - 630 | | |
| $NO_2^+$ | 1400 | | vs | | 570 | | | |
| $FHF^-$ | | 610 - 585 | vs | | 1205 | 1260 - 1200 | m | m |
| $C_{\infty v}$ | | | | | | | | |
| $OCN^-$ | 1292, 1205 | 1215 - 1200 | s | w | 615 | 640 - 600 | | m |
| $SCN^-$ | 745 | | s | w | 470 | 490 - 420 | m | m |
| $C_{2v}$ | | $\nu_s(A_1)$ | | | | $\delta(A_2)$ | | |
| $NO_2^-$ | 1330 | 1380 - 1320 | s | s | 815 | 635 - 825 | m | s |
| $D_{3h}$ | | $\nu_s(A_1')$ | | | | $\rho(A_2'')$ | | |
| $BO_3^{3-}$ | 910 p | 1000 - 925 | vs | | 700 | 760 - 680 | | s |
| $NO_3^-$ | 1050 p | 1060 - 1020 | vs | | 825 | 835 - 780 | w | s |
| $CO_2^{2-}$ | 1060 p | 1090 - 1050 | vs | | 880 | 890 - 850 | | m |
| $C_{3v}$ | | $\nu_s(A_1)$ | | | | $\rho(A_1)$ | | |
| $SO_3^{2-}$ | 965 p | 990 - 950 | vs | s | 615 p | 650 - 620 | w | m |
| $ClO_3^-$ | 930 p | 935 - 915 | s | | 625 p | 625 - 600 | | |
| $BrO_3^-$ | 800 p | 805 - 770 | s | | 440 p | 445 - 420 | | |
| $IO_3^-$ | 780 p | 780 - 695 | s | | 390 p | 415 - 400 | | |
| $OH_3^+$ | 3380 - 3280 | | m | vs | 1180 - 1150 | | | |
| $T_d$ | | $\nu_s(A_1)$ | | | | $\rho(E)$ | | |
| $NH_4^+$ | 3040 p | | s | | 1680 | | | |
| $ND_4^+$ | 2215 p | | s | | 1215 | | | |
| $PO_4^{3-}$ | 935 p | 975 - 960 | vs | | 565 | 600 - 540 | w | m |
| $SO_4^{2-}$ | 980 p | 1010 - 970 | vs | | 615 | 680 - 610 | w | m |
| $ClO_4^-$ | 930 p | 940 - 930 | vs | | 625 | | | |
| $IO_4^-$ | 790 p | | vs | | 325 | | | |
| $MnO_4^-$ | 840 p | 860 - 840 | vs | | 430 | | | |
| $CrO_4^-$ | 850 p | 860 - 840 | vs | | 370 | | | |
| $AsO_4^{3-}$ | 810 p | | vs | | 340 | | | |
| $AlH_4^-$ | 1740 p | 1640 | s | s | 800 | 900 - 800 | w | m |
| $BF_4^-$ | 770 p | | vs | s | 525 | | w | s |

| Molecule (puktgrupp) | $\nu_1$ band, $cm^{-1}$ (vibration, symmetry) | | | | $\nu_2$ band, $cm^{-1}$ (vibration, symmetry) | | | |
|---|---|---|---|---|---|---|---|---|
| | in $H_2O$ | powder | R | IR | in $H_2O$ | powder | R | IR |
| $D_{\infty h}$ | | $\nu_{as}(\Sigma^+)$ | | | | | | |
| $NO_3^-$ | 2070 | 2190 - 2010 | | vs | | | | |
| $NO_2^+$ | 2360 | | | vs | | | | |
| $FHF^-$ | 1535 | 1700 - 1400 | | vs | | | | |
| $C_{\infty v}$ | | | | | | | | |
| $OCN^-$ | 2190 p | 2220 - 2130 | s | s | | | | |
| $SCN^-$ | 2065 p | 2160 - 2040 | vs | s | | | | |
| $C_{2v}$ | | $\nu_{as}(B_1)$ | | | | | | |
| $NO_2^-$ | 1230 | 1260 - 1230 | m | vs | | | | |
| $D_{3h}$ | | $\nu_{as}(E')$ | | | | $\delta(E')$ | | |
| $BO_3^{3-}$ | | 1460 - 1240 | | vs | | 680 - 590 | m | m |
| $NO_3^-$ | 1400 | | m | vs | 720 | 740 - 710 | m | w |
| $CO_2^{2-}$ | 1415 | 1495 - 1380 | w | vs | 680 | 740 - 610 | w | m |
| $C_{3v}$ | | $\nu_{as}(E)$ | | | | $\delta(E)$ | | |
| $SO_3^{2-}$ | 950 | 970 - 890 | m | s | 470 | 520 - 470 | s | m |
| $ClO_3^-$ | 980 | 990 - 965 | m | s | 480 | 500 - 460 | | |
| $BrO_3^-$ | 830 | 830 - 800 | m | s | 350 | | | |
| $IO_3^-$ | 825 | 830 - 760 | m | s | 350 | | | |
| $OH_3^+$ | 3380 - 3270 | | m | vs | 1700 - 1600 | | m | s |
| $T_d$ | | $\nu_{as}(T_2)$ | | | | $\delta(T_2)$ | | |
| $NH_4^+$ | 3145 | | | s | 1400 | 1430 - 1390 | | s |
| $ND_4^+$ | 2350 | | | s | 1065 | | | |
| $PO_4^{3-}$ | 1080 | 1100 - 1080 | | s | 420 | 500 - 400 | | |
| $SO_4^{2-}$ | 1100 | 1140 - 1080 | w | vs | 450 | | w | |
| $ClO_4^-$ | 1130 | 1140 - 1080 | | | 460 | | | |
| $IO_4^-$ | 850 | | | | 255 | | | |
| $MnO_4^-$ | 920 | 940 - 880 | | | 355 | | | |
| $CrO_4^-$ | 885 | 915 - 870 | | | 350 | | | |
| $AsO_4^{3-}$ | 810 | | | vs | 400 | | | |
| $AlH_4^-$ | 1740 | 1785 | | vs | 745 | 800 - 700 | s | s |
| $BF_4^-$ | 985 | | s | vs | 355 | | w | s |

# XI.5. Depolarisation ratio

A laser light source gives **plane polarized light**. The polarization plane (or the electric vector of the incident radiation, $\vec{\mathcal{E}}$), lies perpendicular to the optical axis of the spectrometer. The Raman scattering may alter the direction of the polarization plane. This is known as **depolarization**. By measuring the intensity of the scattered light in two polarization directions, parallel with the polarization plane of the incident light, $I_{\parallel}$, and perpendicular to it, $I_{-}$, one can determine the **depolarization ratio** $\rho$ as

$$\rho = \frac{I_{-}}{I_{\parallel}}. \tag{XI.16}$$

The polarization directions are defined in Fig. XI.12.

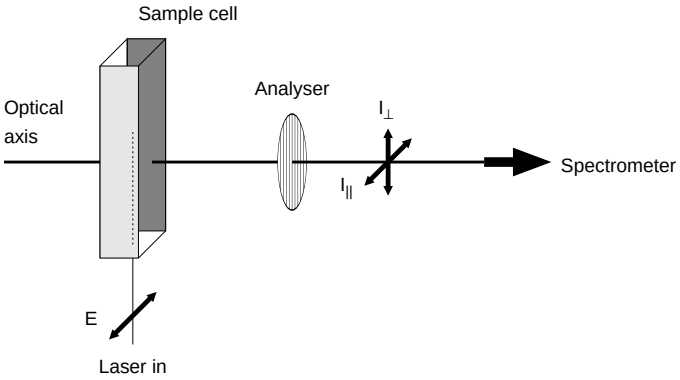


Fig. XI.12. Definition of the parameters for depolarization ratio.

Every band has its characteristic depolarization ratio that depends on the symmetry properties of the vibration. If the vibration belongs to the totally symmetric irreducible representation it will not modify the polarization plane and $\rho = 0$. In that case the vibration is **polarized**. If the vibration is asymmetric it will turn the polarization plane and the depolarization ratio is $\rho = 0.75$. Such vibrations are **depolarized**. Thus the symmetry of the vibration can be deduced from the depolarization ratio. This will help in assignment of the spectral bands.

The spectral bands of carbon tetrachloride at 218 and 314 $\mathrm{cm}^{-1}$ show a depolarization ratio of 0.75. The vibrations belong to the irreducible representations $E$ and $T_2$, respectively, which means that the shape of the molecule changes during the vibration. The vibration observed at 459 $\mathrm{cm}^{-1}$ belongs to the irreducible representation $A_1$ and has a depolarization ratio of 0.006. That vibration does not change the shape of the molecule so the asymmetry of the polarization tensor cannot affect the scattering. The parallel and perpendicular spectra are shown in Fig. XI.13.

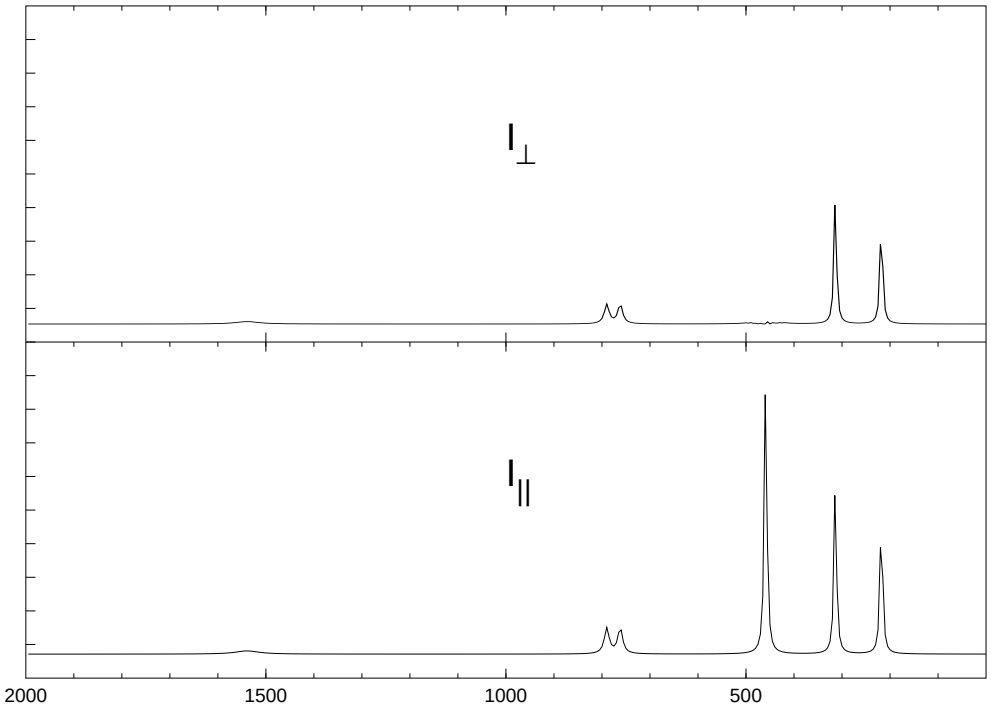


Fig. XI.13. The parallel and perpendicular spectra of carbon tetrachloride.

A more detailed analysis shows that when the incident radiation that propagates in the $z$ direction with $\vec{n}^i = e_z$ = unit vector in $z$ direction the corresponding electric vector lies in $x$ or $y$ direction. The electric vectors are denoted as $E_x^i(\|^i)$ and $E_y^i(-^i)$. Let the incident radiation collide with a molecule that is placed at the origin of the coordinate system. The light scattered at 90° angle will propagate in the direction $\vec{n}^s = e_x$. The momentaneous electric dipole moment emitted by scattering has components $p_z(\|^s)$ and $p_y(-^s)$. The scattered electric vector is parallel with or perpendicular to the scattering plane, in this case $xz$. The coordinate system is shown in Fig. XI.14. One can write the matrix elements of the transition moment in **Placzek's approximation** (*i.e.*, assuming that the polarizability tensor is adiabatic) as

$$\begin{aligned}(p_y) &= (\alpha_{yy})E_y \\ (p_z) &= (\alpha_{zy})E_y\end{aligned} \tag{XI.17}$$

for incident light that is polarized in the $y$ direction.

Consider $N$ freely rotationg ideal gas molecules in the vibrational ground state. Intensity of the scattered light is obtrained by taking the mean value of all orientations, *i.e.*, by replacing $(\alpha_{yy})^2$ by $< (\alpha_{yy})^2 >$. The isotropic mean value is expressed by using invariant quantities that can be defined in several different ways. We use here the quantities (i)

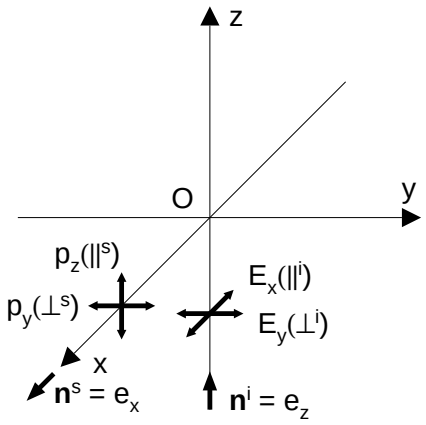


Fig. XI.14. The coordinate system used to define depolarization.

**mean polarizability**[9]

$$a = \frac{1}{3}(\alpha_{xx} + \alpha_{yy} + \alpha_{zz}); \tag{XI.18}$$

(ii) **anisotropy**

$$\begin{aligned}\gamma^2 =& \frac{1}{2}\left\{|\alpha_{xx} - alpha_{yy}|^2 + |\alpha_{yy} - alpha_{zz}|^2 + |\alpha_{zz} - alpha_{xx}|^2\right\} \\ &+ \frac{3}{4}\left\{|\alpha_{xy} + \alpha_{yx}|^2 + |\alpha_{xz} + \alpha_{zx}|^2 + |\alpha_{yz} + \alpha_{zy}|^2\right\};\end{aligned} \tag{XI.19}$$

(iii) **antisymmetric anisotropy**

$$\delta^2 = \frac{3}{4}\left\{|\alpha_{xy} - \alpha_{yx}|^2 + |\alpha_{yz} - \alpha_{zy}|^2 + |\alpha_{zx} - \alpha_{xz}|^2\right\}. \tag{XI.20}$$

The intensity of an oscillating dipole at the angle $\theta$ to the axis of the dipole is

$$I = K_\omega \omega^4 (p)^2 \sin^2\theta. \tag{XI.21}$$

Here only scattering at 90° angle is considered, i.e., $\theta = \pi/2$. Therefore

$$I(\pi/2; -^s, -^i) = K_\omega N \omega^4 < (\alpha_{yy})^2 > E_y^2. \tag{XI.22}$$

Similarly one can obtain the intensity

$$I(\pi/2; \|^s, -^i) = K_\omega N \omega^4 < (\alpha_{zy})^2 > E_y^2. \tag{XI.23}$$

Using the isotropic invariant quantities the intensities can be written as

$$I(\pi/2; -^s, -^i) = K_\omega N \omega^4 \left\{\frac{45a^2 + 4\gamma^2}{45}\right\} E_y^2 \tag{XI.24}$$

[9] For a discussion of the invariant quantities and their relation to the polarizability tensor, see any advanced text book in electrodynamics, or *e.g.* Long.

and

$$I(\pi/2; \|^s, -^i) = K_\omega N \omega^4 \left\{ \frac{\gamma^2}{15} \right\} E_y^2. \tag{XI.25}$$

Using these notations, the depolarization ratio can be written as

$$\rho(\pi/2; -^i) = \frac{I(\pi/2; \|^s, -^i)}{I(\pi/2; -^s, -^i)} = \frac{3\gamma^2}{45a^2 + 4\gamma^2}. \tag{XI.26}$$

# XI.6. Lattice vibrations

**Lattice vibrations** are the molecules' motions with respect to each other in the lattices of a crystalline material. These motions are also quantizised; the quantum number is called a **phonon**. The motions depend on the crystal's symmetry which means that they obey selections rules similar to those for ordinary vibrations.

The masses are high in the lattice vibrations and therefore the motions are slow and the frequencies low. In the infrared spectroscopy they are in the far IR region and are seldomly considered. In Raman spectroscopy they are more easily accessible. The example in Fig. XI.15. shows ammonium perrhenate, $NH_4ReO_4$.[10]

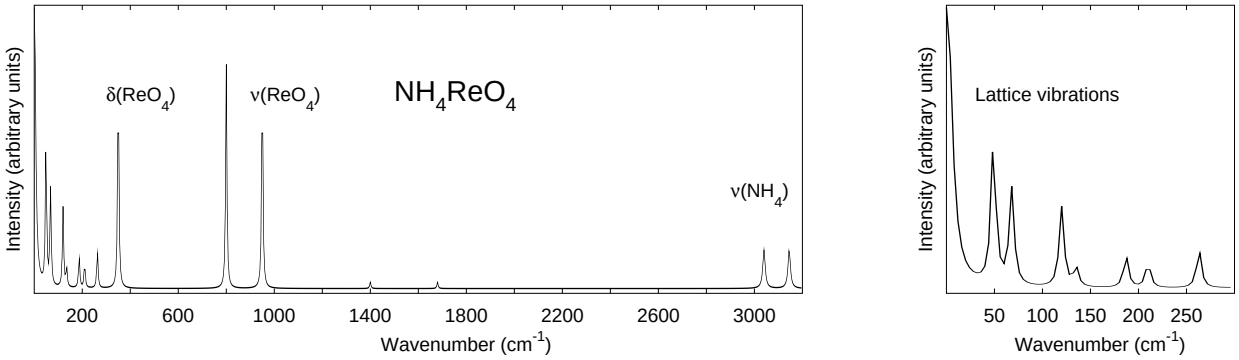


Fig. XI.15. Lattice vibrations in ammonium perrhenate.

[10] Y. S. Park et al., J. Raman Spectr., 17 (1986) 351.

# XI.7. Experimental methods

**Gas samples** are seldomly used in Raman spectroscopy. In thin gases there are normally too few molecules in the focal point of the laser beam. This indicates that lasers with very high power and extremely sensitive detectors must be used. On the other hand many gases absorb only deep in the UV so that incident radiation with quite short wavelengths can be used. This increases of course the scattering cross section.

The highest possible laser intensities are obtained when the sample is placed in the laser cavity.

**Liquid samples** are easily handeled in the Raman experiment. Raman is a form of vibrational spectroscopy so similar rules for the sample as in infrared spectroscopy must be observed. In particular the sample must be a pure compound. Each component of a mixture gives its own set of bands but the interpretation still is quite cumbersome when the number of partly overlapping bands is large.

The sample cells are often nmr tubes or melting point capillary tubes. The glass wall of the cell does not disturb the experiment when the incident light is focused on the sample. The typical incident laser powers range from a few tens to a few hundresd of milliwatts.

The measuring method for liquid samples is normally the 90° geometry but back scattring is also used in some cases.

**powder samples** can in most cases be placed in a capillary or in a cavity on a metal plate. It is also easy to construct sample holders for solid samples, fibres and films so that they can be places in the correct ngle in the spectrometer. The suitable amount of sample depends on how easily handeled the sample is and on the size of the focal point of the incident laser beam, typically approximately 10 $\mu$m.

**Single crystals** can be attached to the $xy$ table of a microscope by using a non-fluorescent glue. By using polarized light and turning the crystal in different orientations it is possible to determine all nine components of the polarization tensor.

**Thin films** can be studied, *e.g.*, by using a sample holder where the light is reflected on the film. One such sample holder is shown in Fig. XI.16. In this way one can obtain perfectly acceptable Raman spectra of 25 Å thick films of long-chained organic molecules, of 75 Å thick phospholipids, of 6 nm thick titanium oxide films or of 1 $\mu$m thick polymer films.

**Strongly absorbing samples** can be problematic because of strong fluorescence or because they are strongly heated. Samples that normally would be combusted by the strong laser light can be placed in a rotating sample holder. Then one has continuously fresh

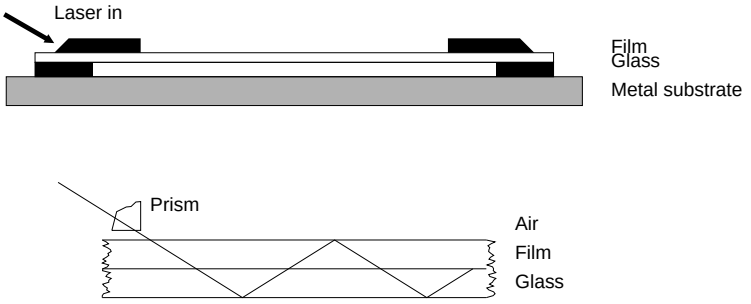





Fig. XI.16. Sample holder for thin films.

sample under the laser beam and the sample does not have time to heat so much that it would be destroyed.

**Raman microscopy** is a popular technique today. The most common method is to place the sample on a $xy$ table and move it so that the laser beam is focused at a network of points on the sample one point at a time. Then one can store the raman spectrum for each point to form a spectroscopic hypercube. One can also illuminate the whole surface at one time and by diffuse light and photograph the surface through a notch filter to see the distribution of strongly scattering molecules on the whole surface. However, one cannot have the spectra and identify the scatterers in this case.

Raman spectroscopy can be used for **quantitative analysis** because the intensity of the emission lines depends linearly on the concentration. It is in fact often easier than in infrared spectroscopy because the calibration curve can be linear in a broader concentration range than in infrared spectroscopy. On the other hand the experimental conditions affect the intensity of the scattered light. It is therefore customary to add an internal reference to the sample in order to eliminate such errors. The accuracy of the quantitative analysis and the limit of determination depend on the scattering cross section of the sample. It has been reported that benzene, which is a strong scatterer, has been analyzed in carbon tetrachloride down to concentrations of ca. 100 ppm. The modern techniques, in particular resonance Raman and SERS, have turned Raman spectroscopy to a sensitive method.

# XI.8. Fluorescence

The purpose of the traditional Raman spectroscopy is that the freauency of the incident light does *not* correspond to any electronic excitation in the molecule. If this happens the light may be absorbed. The possible relaxation processes are then **fluorescence**, or a non-radiative process where the incident power is converted to heat whereby the sample may be destroyed.

Fluorescence is usually a phenomenon to be avoided in Raman spectroscopy. The probability of fluorescence inreases when incident light with a short wavelength is used. Therefore UV or violet/blue/green light is not preferred even though the intensity of the scattered light would be quite high at such frequencies. Instead, infrared light is often used in particular in FT-Raman instruments because of low probability of fluorescence. If fluorescence is observed, its intensity is several decades higher than that of the scattered light and the Raman bands are drowned.

If fluorescence occurs one should, if possible, switch to another laser wavelength. Most often the new wavelength does not coincide with any of the molecule's absorption bands. This is illustrated in Fig. XI.17 where the sample is poly (9-vinylcarbazol) and the two laser wavelengths are 514 and 830 nm.[11]

One common cause of fluorescence is impurities and rest chemicals in the sample. Fluorescence is also a common phenomenon in biochemical and process chemical samples where there are many components. If one can chemically remove the disturbing substances from the sample the fluorescence often vanishes. One may also try to illuninate the sample at high laser power for an extended period of time whereby the disturbing substances are burmed away. This method is called **bleaching**. If the sample itself emits fluorescent light one may try to use a high laser power and see the very weak Raman signals on top of the strong broad fluorescence band.

One should also observe that scattering is an immediate process while fluorescence emission starts several nanoseconds after the incident pulse. A boxcar integrator can therefore separate the raman signal from the fluorescence light.

If the sample **absorbs** and is heated it will be destroyed in a very short time under the intense laser light. The absolutely best method to avoid this is to switch to another laser wavelength that is not absorbed. If this is not possible one should use as low laser power as possible and a short measuring time in order to reduce the heating. One can also **defocus** the incident laser light in order to reduce the energy density. Various **rotating sample holders** have been suggested so that there is constantly fresh sample in the laser focus whereby the heating is minimized. Examples of such sample holders are shown

[11] http://www.k-analys.se

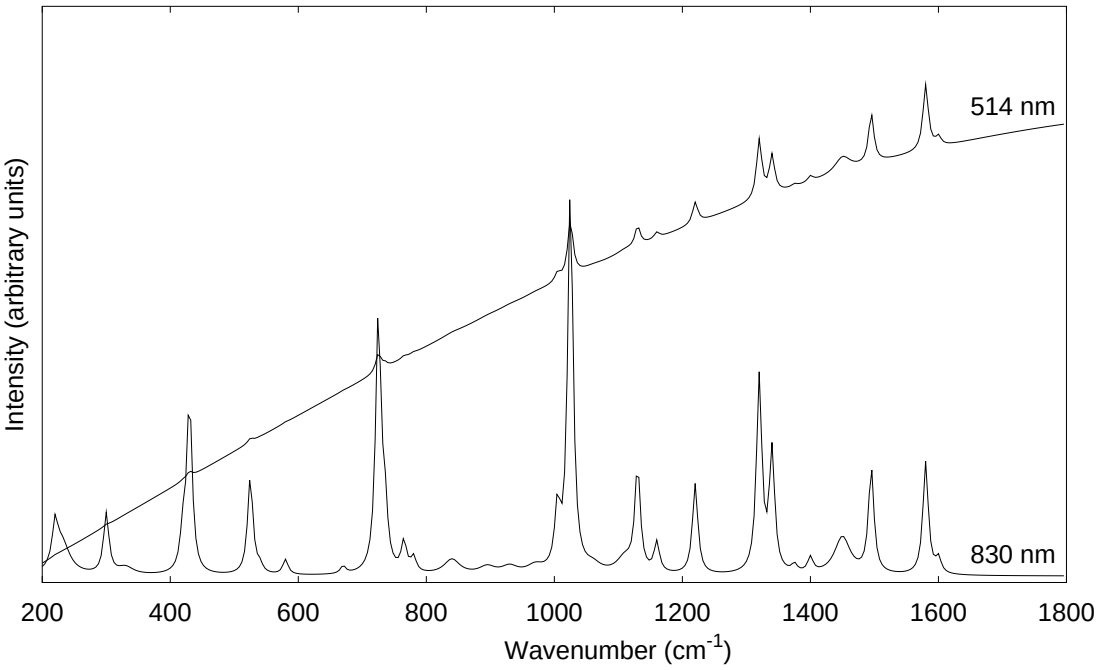


Fig. XI.17. Raman spectrum of poly (9-vinylcarbazol) at two incident laser wavelengths of which one induces fluorescence. The scales for the fluorescence and Raman light are not the same.

schematically in Fig. XI.18. In the first sample holder the powder is pressed to a groove. In the second one the liquid is driven to the edge of the sample holder by the centrifugal force.

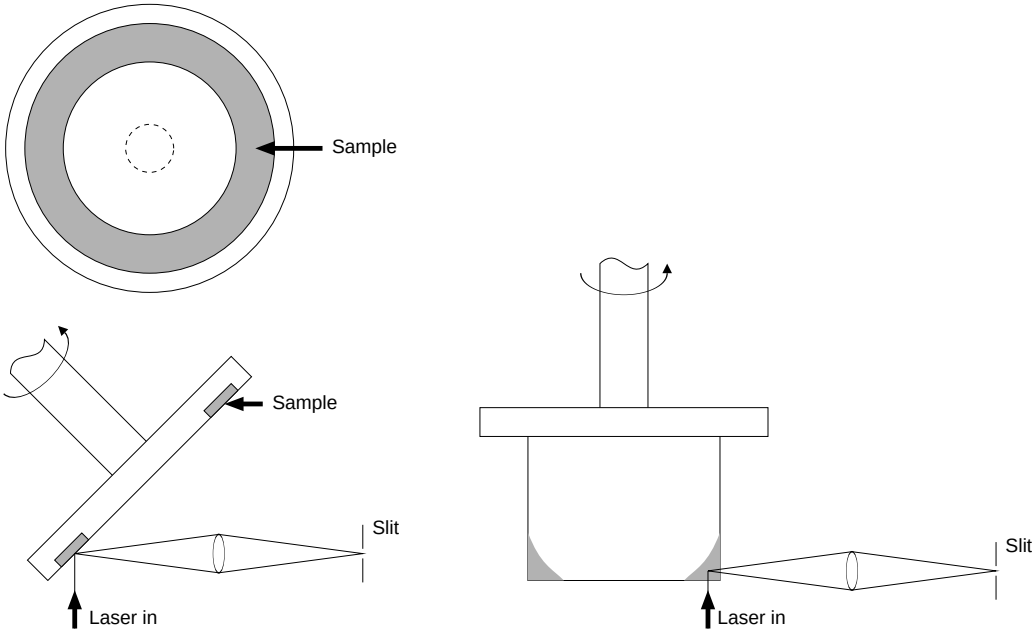


Fig. XI.18. Examples of rotating sample holders for Raman spectroscopy. The first one is intended for powder samples and the second for liquid samples.

## XI.9. Resonance Raman spectroscopy

Sometimes one can deliberately choose to use a laser wavelength that will induce fluorescence. Such a method is known as **resonance Raman spectroscopy**. In resonance Raman spectroscopy the intensity of the Raman signal is increased by a factor of $10^2$ - $10^6$. This is a particularly useful technique for biochemical or process chemical samples that are mixtures of a number of substances. In such samples one can select one particular component that absorbs at the laser wavelength that is used. *E.g.*, the active centre of an enzyme often contains a metal ion that gives the complex a visible color while the rest of the organic material does not absorb. In that case one can obtain the Raman spectrum of just the active centre and nothing else. At the same time one can obtain information of the electronic state of the active complex.

The enhancment affect exactly those parts of the molecule where the electronic absorption takes place. Not all vibrations of the molecule are enhanced equally much. If one uses, *e.g.*, the wavelength of an electronic $\pi^* \leftarrow \pi$ transition the Raman signal of the stretching vibration of the $\pi$ bond will be affected most. Similarly, the vibrations of the metal-ligand bonds will be enhanced if the incident wavelength is adjusted to the absorption band of the metal complex. The Raman spectrum and resonance Raman spectrum of para-ethyl phenols (PEP) in hexane are shown in Fig. XI.19. The Raman spectrum was produced using laser light with 514 nm wavelength and the resonance Raman spectrum with 244 nm. The spectral bands of PEP are marked with strokes. The most important bands

of the solvent are marked with stars. Their intensity is not affected very much by the resonance.[12]

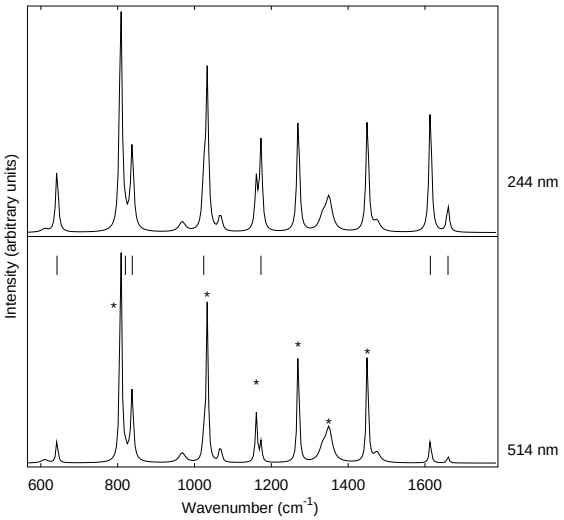


Fig. XI.19. Raman and resonance Raman spectra of para-ethyl phenol.

The origin of the enhancement can be read in the first term of the Kramers-Heisenberg equation where the energy denominator contains the difference of frequencies (see Appendix I). This difference becomes small when the laser wavelength lies close to an absorption band.

[12] M. P. Russel et al., Biophys. J., 68 (2995) 1607.

# XI.10. SERS

In **surface Enhanced Raman Scattering**, **SERS**) the sample is placed on a metal surface with an ordered crystal lattice. In this case the intensity of Raman scattering will be increased by a factor of $10^3$ - $10^6$ as compared to liquid samples. A silver surface gives the best results even though other metals, gold in particular, can also be used.

The phenomenon is explained by the fact that the easily polarizable conduction electrons enhance the electric field of the incident light that a molecule in the sample feels. It has also been claimed that the molecules or ions on the metal surface can form weakly bonded electron transfer complexes which have an absorption band at the laser wavelength. This would then lead to a resonance enhancement.

As an example consider the surface enhanced Raman spectrum of trans-1,2-bis(4-pyridyl)-ethylene (BPE) that is a relatively strong Raman scatterer. The spectrum is shown in Fig. XI.20. The spectrum has been created by using a frequency doubled Nd:YAG laser beam at 532 nm. The laser effect was 1.5 mW and the measuring time 5 s.[13]

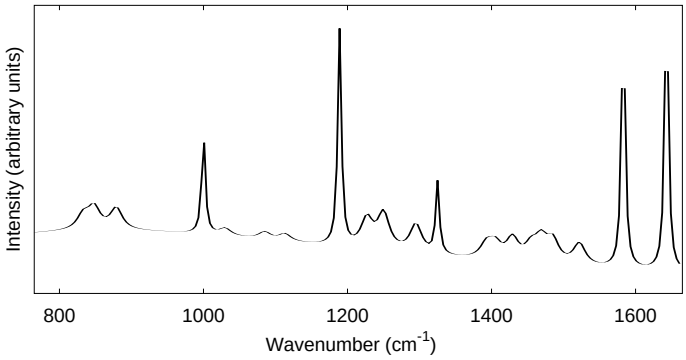


Fig. XI.20. The surface enhanced Raman spectrum of BPE on a AgFON silver surface.

[13] M. A. Young et al., *Can. J. Chem.*, **82** (2004) 1435.

# XI.11. CARS

Two lasers are used in the **Coherent Anti-Stokes Raman scattering**, **CARS**). One of them has a fixed frequence $\nu_1$ and the other is a dye laser or another laser light source with adjustable frequency $\nu_2$. The first laser gives rise to a normal Raman phenomenon. At the same time the sample is also illuminated with the second laser that sweeps over the whole anti-Stokes-Raman spectrum. When the frequency of the dye laser coincides with a Raman transition the two intense electric fields will interact and a strong scattered laser beam with the frequency $\nu_3 = 2\nu_1$ - $\nu_2$ will be emitted. This phenomenon is based on the **non-linear optics**. In principle, the two laser beams should be aligned accurately so that the electric vectors meet at the correct angle. However, for siquid samples the beams can usually be parallel. The experimental setup is shown schematically in Fig. XI.21.

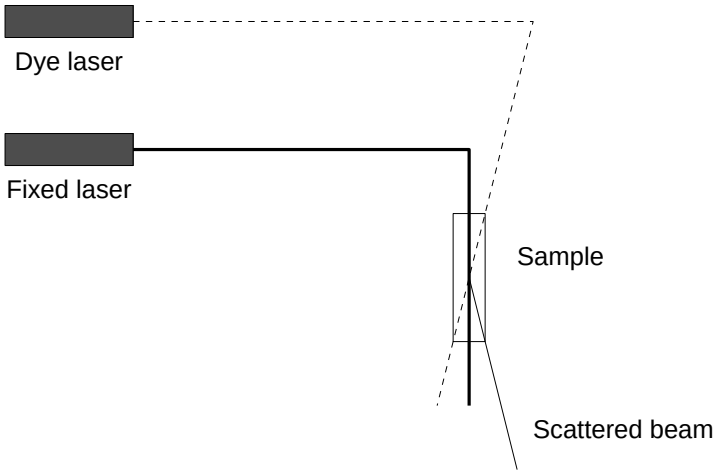


Fig. XI.21. The CARS experiment schematically.

The CARS technique is suitable also for samples with strong disturbances such as fluorescence. One important field of application is the vibration spectroscopy of molecules in flames.

A more detailed illustration of the principle of CARS spectroscopy is shown in Fig. XI.22a. The two laser beams $\nu_1$ and $\nu_2$ interact and create the two virtual states $\mid a >$ and $\mid b >$ that co-exist and are in coherence. The whole process involves four photons and is based on the third order **hyperpolarizability** $\chi^{(3)}_{\sigma\tau\nu}$. The momentaneous induced dipole moment of the molecule is

$$p_\lambda = \mu^0_\lambda + \sum_\sigma \alpha_{\lambda\sigma}\mathcal{E}_\sigma + \frac{1}{2}\sum_{\sigma\tau} \beta_{\lambda\sigma\tau}\ \mathcal{E}_\sigma\mathcal{E}_\tau + \frac{1}{6}\sum_{\sigma\tau\nu} \epsilon_0\chi^{(3)}_{\sigma\tau\nu}\mathcal{E}_\sigma\mathcal{E}_\tau\mathcal{E}_\nu. \qquad \text{(XI.27)}$$

Here $\mu^0_\lambda$ is the molecule's permanent static dipole moment, $\alpha_{\lambda\sigma}$ polarizability (or the linear electric susceptibility $\chi^{(1)}_{\sigma\tau}$ multiplied with $\epsilon_0$) and $\beta_{\lambda\sigma\tau}$ is the first hyperpolarizability. The

quantity $\mathcal{E}_\sigma$ is a component of the external oscillating electric field. The CARS method is based on the third order **non-linear optics**. In addition, the wave vectors of the incident and departing beams must fulfil the sum rule of Fig. XI.22b.

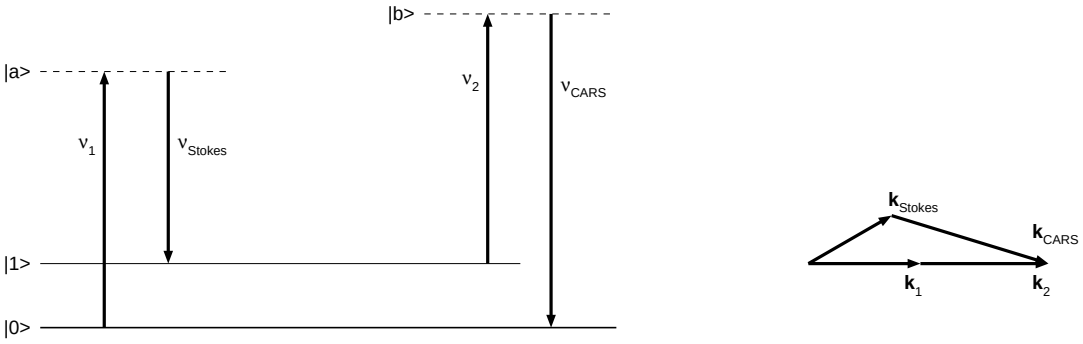


Fig. XI.22. (a) Energy levels in the CARS experiment; (b) sum rule of the wave vectors.

CARS is today available also in microscopy and in mapping teqchniques. Time-dependent CARS has also been reported.

# XI.12. Time-resolved Raman spectrooscopy

Fast phenomena can be observed by sending short laser pulses to the sample. The pulse characteristics and the speed of the detcting assembly determine how short-lived processes can be observed. In specialized laboratories one can reach a time scale of femtoseconds.